

Photocatalytic Degradation of Methyl Orange Dye using Cr-doped ZnS Nanoparticles under Visible Radiation

Alemseged Eyasu, O.P.Yadav* and R.K.Bachheti

¹Chemistry Department, Haramaya University, Post Box: 138, Dire Dawa, Ethiopia

*Corres. author: yadavop02@yahoo.com

Abstract: Chromium doped ZnS nanoparticles, with 0.05, 0.1, 0.2 and 0.3 mol % of Cr have been prepared using incipient wetness impregnation method. As-synthesized Cr-ZnS composite was characterized using UV-visible spectroscopy and XRD techniques. Kinetics of photocatalytic degradation of methyl orange (MO) dye catalyzed by synthesized nanoparticles was studied under UV and visible radiation. Effect of parameters such as dopant concentration, pH, and dye initial concentration on the photocatalytic degradation of MO dye were investigated. Photocatalytic degradation decreased with increasing dye initial concentration. Using 0.2 mol % Cr-ZnS as photocatalyst, the dye was degraded 74.28% and 65% under visible and UV radiation, respectively, at 5 hrs of the reaction. Higher photocatalytic degradation of dye under visible radiation than under UV radiation is attributed to red-shift of the absorption edge of the Cr-doped ZnS photocatalyst enabling it to harvest more photons in the visible light

Keywords: degradation; kinetics; methyl orange; spectroscopy; visible.

Introduction

Environmental problems associated with hazardous wastes and toxic water-pollutants have attracted much attention. Organic dyes are one of the major groups of pollutants in wastewaters released from textile and other industrial processes. Among various Physical

and biological techniques for the treatment of pollutants, precipitation, adsorption, air stripping, flocculation, reverse osmosis, and ultra-filtration can be used for color removal from textile effluents(1). These techniques are non-destructive and merely transfer the non-biodegradable matter into sludge, giving rise to new type of pollution, which needs further treatment (2). Recently, there has been considerable interest in the utilization of advanced oxidation processes (AOPs) for the complete destruction of dyes.

Heterogeneous photocatalysis, one of the advanced oxidation processes (AOPs), is a cost-effective treatment method for the removal of toxic pollutants from industrial waste water owing to its ability to convert these into safer end products such as CO₂, H₂O, and mineral acids (3,4). Semiconductor nanoparticles, as heterogeneous photocatalysts, have attracted much interest due to their size tunable physical and chemical properties. Transition of matter from bulk to nanosize, displays quantum mechanical properties and increased dominance of surface atoms, which give rise to unique photo-physical and photo-catalytic properties to the nanomaterial. Such differences in the photocatalytic activity are related to the variations in the surface impurities, existence of structural defects into crystalline framework or density of hydroxyl groups on the catalyst's surface (5). Transition-metal sulphides have unique catalytic functions due to rapid generation of electron-hole pairs by their photo-excitation and the highly negative reduction potentials of excited electrons (6,7). Further, incorporation of transition metal ion dopants in these semiconductor nanoparticles, can influence their photo-catalytic performance. The effect of metal doping on the activity of a photocatalyst is governed by

several factors such as: the nature and amount of the dopant, preparation method and the initial concentration of the pollutants to be treated

Though several modification techniques for improving the photocatalytic activity of semiconductor photocatalysts have, earlier, been reported, little work appears on the transition metal doping and no work is reported on the kinetic study of degradation of methyl orange dye using nanosize Cr-doped ZnS as photocatalyst. We report, here, the kinetics of photocatalytic degradation of methyl orange dye using as-synthesized Cr-doped ZnS nanoparticles as photocatalyst. Effects of dopant (Cr) concentration in Cr-ZnS photocatalyst, pH and dye initial concentration on the degradation of methyl orange (MO) have been reported..

2. Materials And Methods

2.1. Materials

ZnSO₄.5H₂O, Na₂S.7H₂O, Cr(NO₃)₃.9H₂O, and methyl orange. NaOH, HCl, and isopropanol used were of analytical grade. spectrophotometer (Model: SP 65; X-Ray diffractometer ((BRUKER D8 Advance XRD, AXS GMBH, Karlsruhe, West Germany)-

2.2. Methods

2.2.1 Synthesis of ZnS Nanoparticles

One molar solution of sodium sulphide was added drop wise into one molar zinc sulphate solution under continuous stirring at 400 rpm until the white precipitates formed The suspension was filtered and the precipitates were washed several times with distilled water, dried at 100 °C for 24 hours and grinded to achieve fine powder.

2.2.2. Synthesis of Cr -doped ZnS nanoparticles

Appropriate amount of Cr(NO₃)₃.9H₂O was dissolved in distilled water by stirring at 400 rpm for 5 minutes. As-synthesized ZnS powder was mixed in the above solution by agitating for one hour. The product was filtered and washed 3 times with distilled water until the filtrate was free of nitrate ions. The product was dried at 105°C for 24 h and grinded to fine powder and finally calcinated at 300°C for 4 hours. Chromium doped Zinc sulphide (Cr_xZnS_{1-x}) (x= 0.05, 0.1, 0.2 and 0.3 mol%) composite photocatalyst samples were prepared.

2.2.3 UV-Visible Absorption Study

The UV-visible absorption spectra of the as-synthesized photocatalysts, dispersed in isopropanol, over 200-800 nm was obtained using a spectrophotometer (Model: SP 65); X-ray diffractometer

2.2.4. XRD Analysis of Photocatalyst

XRD analysis of 0.2 mol % of Cr-ZnS photocatalyst sample was carried out using a X-ray diffractometer equipped with Cu K radiation ($\lambda = 0.15406$ nm) source. The diffraction patterns were recorded in the range $2\theta = 4$ to 64° with 0.02° step size and an acquisition time of 1s/step.

2.2.5. Photocatalytic Dye Degradation Study

To 100 ml of dye solution, a known amount of photocatalyst was mixed in a cylindrical pyrex reactor of 500 ml capacity (Fig.). It was magnetically stirred under dark for 30 minutes to attain adsorption equilibrium between the adsorbent (Cr-ZnS) and the adsorbate (dye solution). Irradiation under UV or visible light was done upto 180 minutes. Five ml each of the reaction mixture was collected at 30 minutes interval of time and its absorbance at 465 nm was recorded using a UV-Visible spectrophotometer.

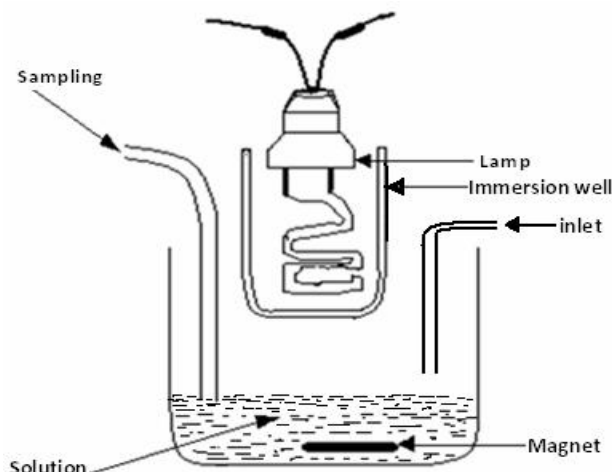


Fig. 1. Photocatalytic Reactor

3. Results And Discussion

3.1. XRD analysis

XRD pattern of 0.2 mole% Cr-doped ZnS photocatalyst is presented in Fig. 2.

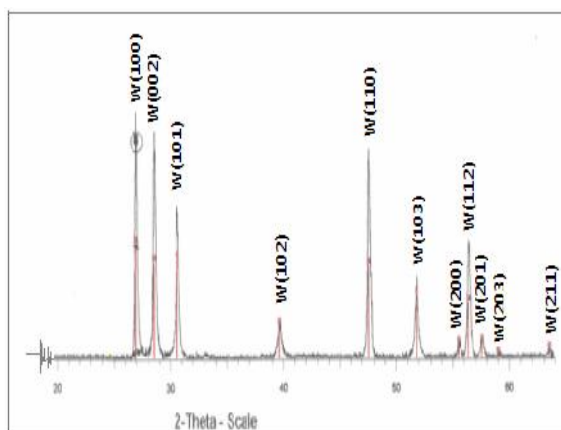


Fig. 2. XRD pattern of Cr(0.2 mol %)- ZnS nanoparticles.

The observed XRD diffraction peaks at $2\theta = 27, 28.5, 30.7, 39.7, 47.5, 51.8, 55.5, 56.4, 57.7, 59.3$ and 63.7 originate from (100), (002), (101), (102), (110), (103), (200), (112), (201), (203), and (211) planes, respectively, from hexagonal wurtzite phase (W) of pure ZnS (8,9). Absence of extra peaks due to impurities indicate high purity of the synthesized photocatalyst.

The average crystallite size of Cr-doped ZnS was determined from Debye–Scherrer formula Lv et al. (10)

$$D = 0.94 \cdot \lambda / (\Delta 2\theta \cdot \cos \theta) \quad (1)$$

Where, D is average size of particle; λ is the X-ray wavelength ($=0.15406$ nm), $\Delta 2\theta$ is full width at half-maxima of diffraction peak (at $2\theta = 27^\circ$); and θ is the angle of diffraction with geometric factor equal to 0.94. The average crystallite size of the Cr(0.2 mol %)-ZnS composite photocatalyst sample was found to be 41.5 nm.

3.2 UV–Vis absorption spectra of Photocatalyst

UV-visible absorption spectra of ZnS and Cr(0.2 mol %)- ZnS photocatalysts, dispersed in isopropanol, are presented in Figure 4. The absorption edge for the above photocatalysts were found to be at 325 and 418 nm, respectively. The red shift in the absorption edge for Cr- ZnS nanoparticles is related to the band gap decrease of ZnS when Cr is doped into ZnS.

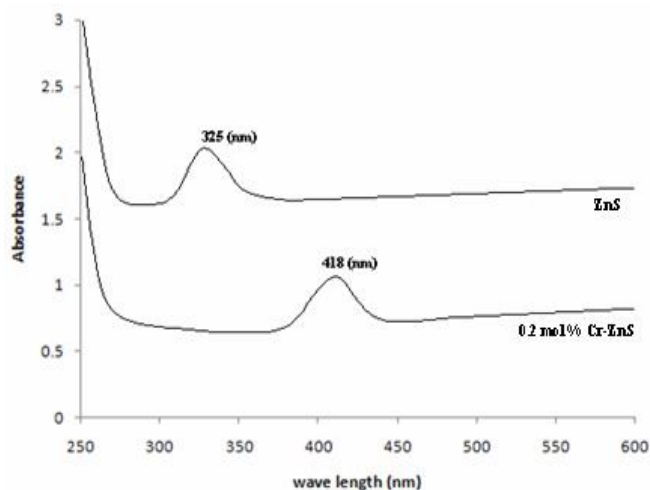


Figure 3. UV-visible spectra of ZnS and Cr(0.2 mol %)-ZnS photocatalyst dispersed in isopropyl alcohol.

The band gap energy (E_g) of as-synthesized photocatalyst was calculated using the equation:

$$E_g \text{ (eV)} = 1240 / \lambda \quad \text{------(2)}$$

Where, E_g is band gap energy (in electron volts), and λ is the wavelength (nm) at the absorbance maxima. The band gap energy for pure ZnS and Cr(0.2 mol %)-ZnS nanoparticles are 3.82 and 2.97 eV, respectively. It is evident that the Cr-ZnO composite should be photocatalytic active in the visible light.

3.3 Photocatalytic Degradation of Methyl Orange under visible radiation

Percent photocatalytic degradation (%D) of methyl orange (MO) dye was calculated using the relation (11)

$$\%D = (1 - A_t/A_0) \times 100 = (1 - C_t/C_0) \times 100 \quad \text{----- (3)}$$

Where A_0 and A_t are the absorbance of dye solution at the initial stage and at time 't' of the reaction, respectively and C_0 and C_t are the corresponding dye concentrations, respectively.

3.4 Effect of dye initial concentration on photo-catalytic degradation

Plots of % photocatalytic degradation of MO as a function of irradiation time (in hr) at varying dye initial concentration (10×10^{-5} to 75×10^{-5} M) using fixed amount (0.5 g /100 ml) of catalyst ($\text{Cr}_{(0.2\text{mol}\%)}\text{-ZnS}$) are presented in Fig.4. Photocatalytic degradation of the dye decreases with the increase in its initial concentration.

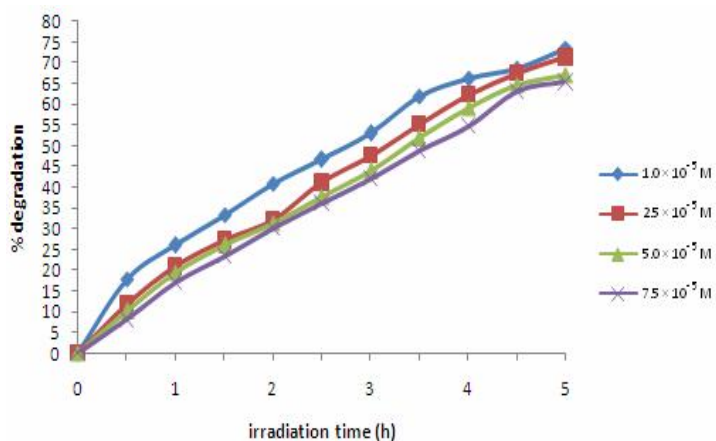


Fig. 4. Plots of % photocatalytic degradation of MO under visible radiation as a function of irradiation time (in hr) at varying dye initial concentration using fixed amount (0.5 g /100 ml) of catalyst ($\text{Cr}_{(0.2\text{mol}\%)}\text{-ZnS}$) and pH(=7)

3.5. Effect of dopant concentration in ZnS on photocatalytic degradation of dye

0.05g of each xCr-ZnS ($x = 0.00, 0.05, 0.1, 0.2,$ and 0.3 mol % of chromium content) samples were taken in different Erlenmeyer flask each containing 2.5×10^{-4} M MO at pH 7. The mixture was stirred for 30 min in dark to achieve adsorption equilibrium and was then irradiated with visible light for 5 hrs. Five ml each of reaction mixture was collected at regular interval of time; suspended particles, if any, were removed by centrifugation. Absorbance and the concentration of dye were determined, spectrophotometrically. Plots of percent photocatalytic degradation of dye as a function time at different dopant concentration using the composite photocatalyst Cr-ZnS are presented in Fig. 5. Plot of % photocatalytic degradation of MO on Cr-ZnS photocatalyst vs. dopant concentration at 5 h is shown in Fig. 6.

Initially, percent photocatalytic degradation of dye increased with the increase of dopant concentration upto 0.2mol %. At still higher dopant concentration, however, the dye degradation decreased. Using 0.2 mol % Cr in ZnS, photocatalytic degradation of dye was 71.28%, whereas, using pure ZnS powder as photocatalyst only 63.19% degradation of the dye was observed. Higher photo-catalytic degradation of dye using Cr doped-ZnS compared to pure ZnS may be due to trapping photo-excited electrons at conduction band by the doped Cr, thereby decreasing the electron-hole recombination.

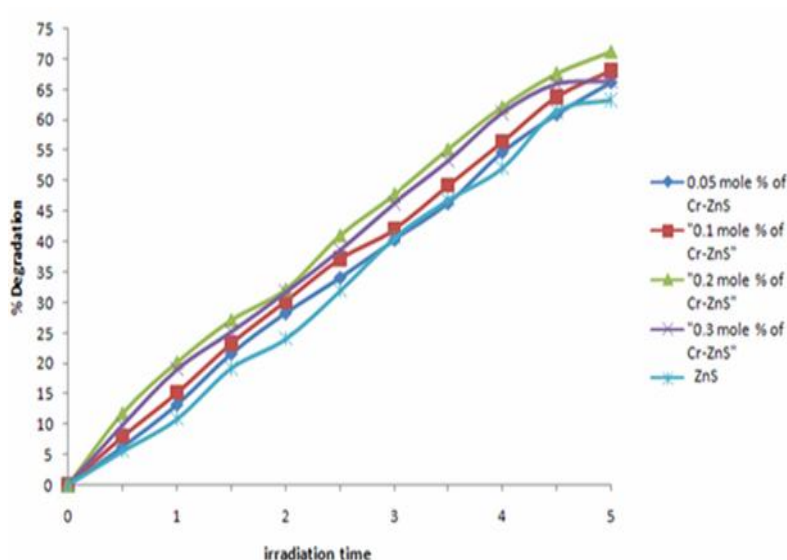


Fig. 5. Plots of % photocatalytic degradation vs. irradiation time (hr) under visible light using different dopant concentration in xCr-ZnS (x in mole %) of Cr photocatalyst with fixed MO concentration (2.5×10^{-4} M) at pH 7.

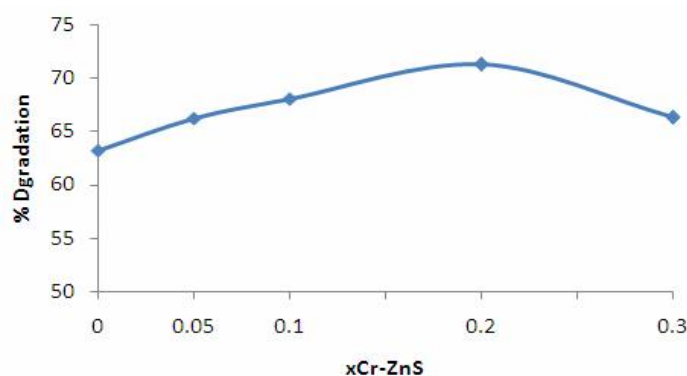


Figure 6 .Plot of % degradation of MO vs. dopant concentration (x in mol%) at 5 h over using xCr-ZnS photocatalyst.

3.6. Effect of pH on MO Photocatalytic Degradation

Plots of percent degradation of MO as a function of time at various pH using MO initial concentration = 2.5×10^{-5} M and optimum catalyst load (0.05 g of 0.2 mol % of Cr-ZnS) are presented in Figure 7 and such plots for degradation of dye at 5h irradiation time for the above system is given in Figure 8. It is observed that % degradation of MO increases when pH is raised from 2 to 3 but at still higher pH the degradation of the dye is gradually decreased. Degradation of the dye remains almost invariant in the pH 3 to 7. Above pH, 7, the photocatalytic degradation of MO rapidly decreases. This may be due to the existence of negative charge at ZnS photocatalyst due to the adsorbed OH⁻ ions at its surface since the point of zero charge (Pzc) of ZnS is pH = 7 (12) and the adsorption of negatively charged MO at the photocatalyst surface is unlikely (13) and hence a decrease in the observed photocatalytic degradation.

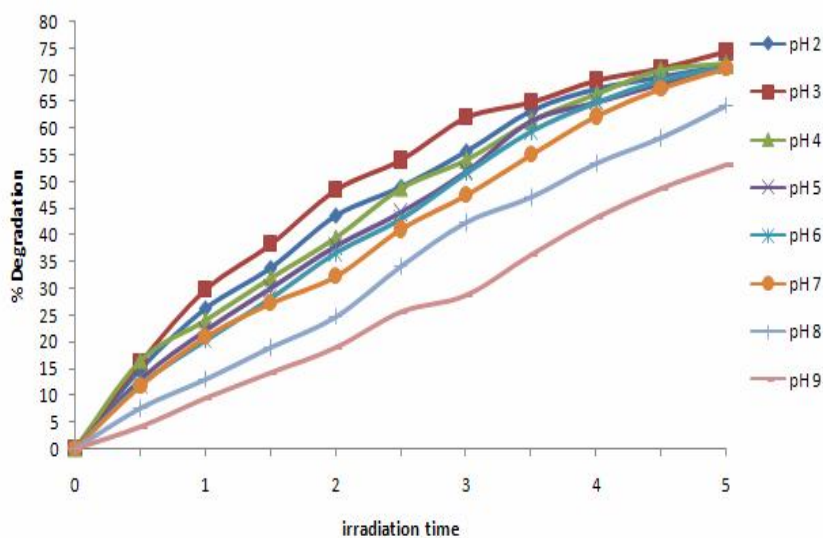


Figure 7. Plots of % degradation vs. irradiation time (h) for degradation of MO aqueous solution under visible radiation at various pH. MO initial concentration = 2.5×10^{-5} M and optimum load of photocatalyst Cr-ZnS = 0.05 g/litre (containing 0.2 mol % Cr)

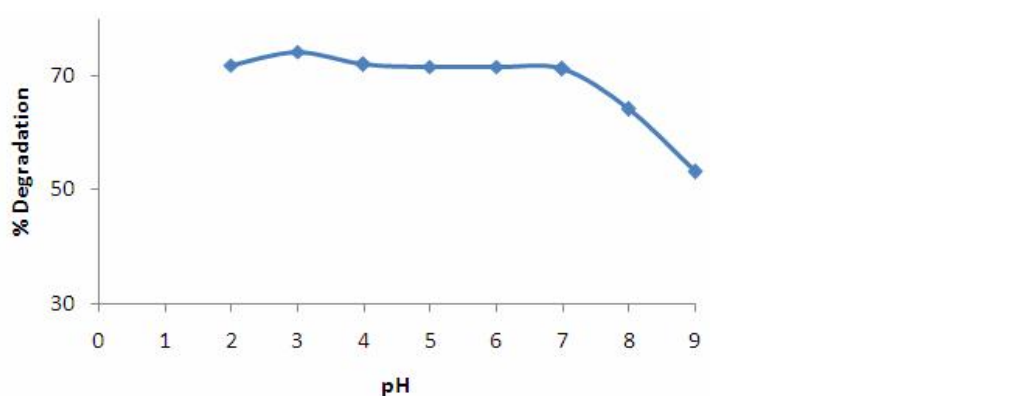


Figure 8. Plot of % degradation vs. pH at 5h irradiation time for degradation of MO aqueous solution at various pH. MO initial concentration = 2.5×10^{-5} M and optimum load of photocatalyst Cr-ZnS = 0.05 g/litre (containing 0.2 mol % Cr).

3.7. Effect of dopant concentration in ZnS photocatalyst on Kinetics of photocatalytic Degradation of Dye

Photocatalytic degradation rate constant (k) of the MO dye was calculated using Langmuir-Hinshelwood first order kinetics (3).

$$\ln C_0/C_t = k.t \quad \text{-----} \quad (4)$$

Where, C_0 and C_t are the concentrations of dye at initial stage and at time t , respectively.

Plots of $\ln C_0/C_t$ vs. irradiation time (in hr) for photocatalytic degradation of MO over composite photocatalyst $\text{Cr}_x\text{-ZnS}$ with different molar concentration of dopant (Cr) using 2.5×10^{-4} M MO initial concentration and pH 7 are presented in Figure-9 and the plot of observed rate constant rate (k in hr^{-1}) as a function of dopant concentration in $\text{Cr}_x\text{-ZnS}$ for photodegradation of MO is presented in Figure 10. Initially, photocatalytic degradation rate constant (k) increased with increasing dopant concentration upto 0.2 mol % and then decreased at higher dopant concentration. Ionic radii of Cr^{+3} and Zn^{+2} being 0.63 Å and 0.74 Å, respectively, the doped Cr^{+3} can enter ZnS lattice substitutionally (14,15). Doped Cr^{+3} upto an optimal concentrations in ZnS acts as trap for photo-excited electrons that lengthens the lifetime of charge carriers results in enhanced photocatalytic activity of ZnS. However, at higher dopant Cr^{+3} concentration, the charge carriers may recombine through quantum tunneling leading to a decreased photocatalytic activity of Cr-ZnS (7).

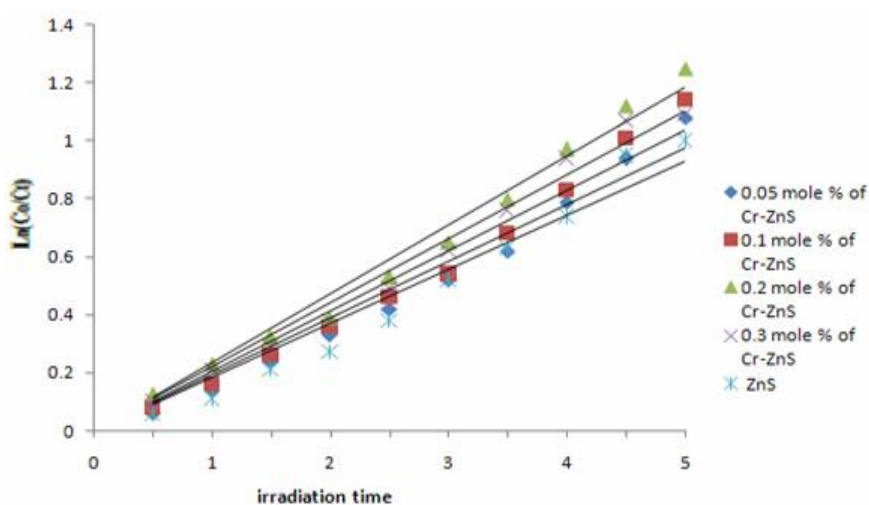


Figure 9. Plots of $\ln C_0/C_t$ vs. irradiation time (in hr) for photocatalytic degradation of MO over composite photocatalyst $\text{Cr}_x\text{-ZnS}$ with different molar concentration of dopant (Cr) using 2.5×10^{-4} M MO initial concentration and pH =7.

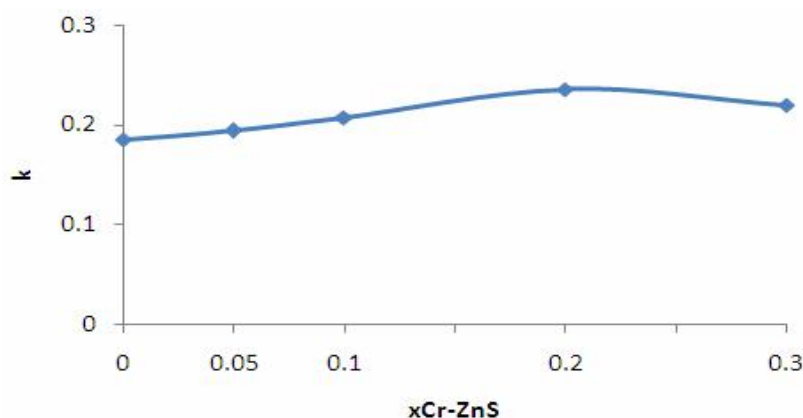


Figure 10. Plot of photocatalytic degradation rate constant (k , in hr^{-1}) of MO as a function of dopant concentration in $\text{Cr}_x\text{-ZnS}$ ($x = \text{mol\% of Cr}$) under visible radiation.

3.8. Comparison of Photocatalytic Degradation of MO under UV and visible radiation

Plots of photocatalytic degradation of MO under UV and visible radiation as a function of time using 0.5g/100ml $\text{Cr}_x\text{-ZnS}$ ($x = 0.2$ mol % Cr) photocatalyst, dye initial concentration 2.5×10^{-4} M and pH =7 are presented in figure 10. Percent photocatalytic degradation of MO is higher under visible light than under UV

radiation. At 5 hrs of reaction time maximum degradation of MO under visible and UV radiation were 71.28 % and 65.22 %, respectively.

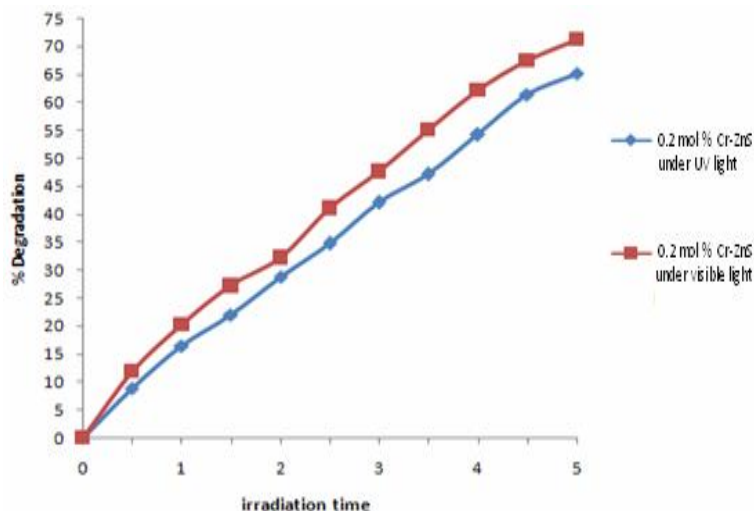
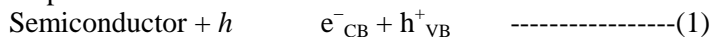


Figure 10. Plots of photocatalytic degradation of MO under UV and visible radiation as a function of time using 0.5g/100ml Cr_x-ZnS (x=0.2 mol % Cr) photocatalyst, dye initial concentration 2.5×10^{-4} M and pH=7.

4. Mechanism of photocatalysis at Cr- ZnS surface

Degradation of dye at the photocatalyst (Cr-ZnS) involves the following steps-

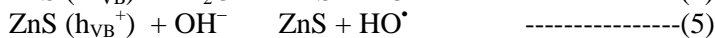
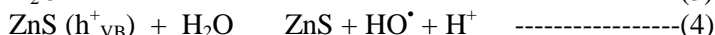
Step-1: Photo-excitation of semiconductor valence band electron creating hole (h^+) and free electron (e^-)-



Step-2: Conversion of photocatalyst surface- adsorbed oxygen to form superoxide radical ($O_2^{\cdot-}$)



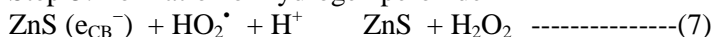
Step-3: Formation of HO^{\cdot} radicals by the reaction of valence band hole (h^+_{VB}) with adsorbed H_2O or HO^- ions-



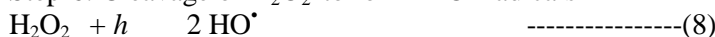
Step-4: Neutralization of superoxide radical ($O_2^{\cdot-}$) by protonation forming HO_2^{\cdot} radical-



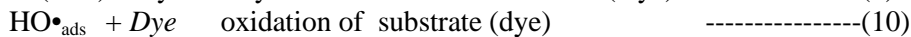
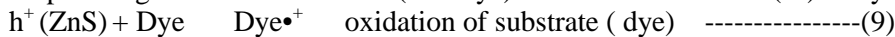
Step-5: Formation of hydrogen peroxide-



Step-6: Cleavage of H_2O_2 to form HO^{\cdot} radicals



Step-7: Degradation of substrate (MO dye) of valence band hole (h^+) or by HO^{\cdot} radical-



Various reaction involved in the photocatalytic degradation of dye at Cr-ZnS surface are also displayed in Figure-11.

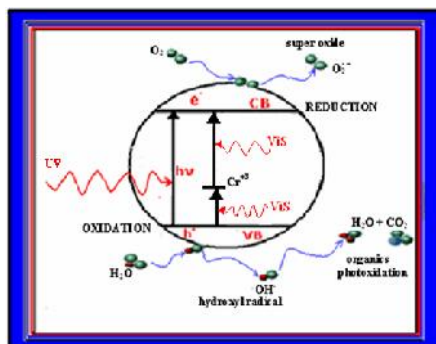


Figure11. Reactions involved in the photocatalytic degradation of dye at Cr-ZnS surface under UV/Visible radiation

4. Conclusion

Chromium doped ZnS nano-size semiconductor photocatalysts i.e. $x\text{Cr-ZnS}$ ($x = 0.05, 0.1, 0.2 \text{ \& } 0.3 \text{ mol\%}$) have been synthesized using incipient wetness impregnation method. The hexagonal wurtzite phase with optimum dopant was characterized using XRD and UV-visible spectroscopic techniques. Effect of dopant (Cr) concentration in Cr-ZnS, dye initial concentration and solution pH on photocatalytic degradation of methyl orange dye under visible radiation were studied. Whereas, degradation of the dye decreased with the increase of dye concentration over the studied concentration range, optimum dopant concentration (0.2 mol %) and optimum pH (= 3.0) were required for highest dye degradation.

Acknowledgments

The Authors express their gratitude to Tigray Education Bureau, Ministry of Education (Ethiopia) for financial support and Haramaya University as well as Addis Ababa Geological Survey for providing Laboratory facilities.

References

1. Robinson, T., G. McMullan, R. Marchant & P. Nigam, Remediation of dyes in textile effluent: a critical review on current treatment technologies with a proposed alternative, *Bioresource Technology.*, 2001, 77, 247-255.
2. Arslan, I., A. Balcioglu, T. Tuhkanen & D. Bahnemann, 2000. $\text{H}_2\text{O}_2/\text{UV-C}$ and $\text{Fe}^{2+}/\text{H}_2\text{O}_2/\text{UV-C}$ versus $\text{TiO}_2/\text{UV-A}$ treatment for reactive dyewastewater, *Journal of Environmental Engineering.* 126: 877-903.
3. Ollis, D.F. & C. Turchi., Heterogeneous photocatalysis for water purification: Contaminant mineralization kinetics and elementary reactor analysis, *Journal of Environmental Programs.*, 1990, 9, 229-234.
4. Kato S, Y., M. Hirano, T. Iwata, K. Sano, T. Takeuchi & S. Matsuzawa., Photocatalytic degradation of gaseous sulphur compounds by silver-deposited titanium dioxide, *Journal of Applied Catalysis of Environmental Biology.*, 2005, 57: 109-115.
5. Qamar, M., M. Saquib & M. Muneer., Photocatalytic degradation of two selected dye derivatives, chromotrope 2B and amido black 10B, in aqueous suspensions of titanium dioxide, *Journal of Dyes and Pigments.*, 2005, 6, 1-10.
6. Stroyuk, A.L., A.E. Raevskaya, A.V. Korzhak & S.Y. Kuchmii., Spectral properties and photocatalytic activity in metals reduction reactions of zinc sulfide nanoparticles. *Journal of Nanoparticles.*, 9, 1010-1027.
7. Pouredal, H. R. & M. H. Keshavarz., Study of Congo red photodegradation kinetic catalyzed by $\text{Zn}_{1-x}\text{Cu}_x\text{S}$ and $\text{Zn}_{1-x}\text{Ni}_x\text{S}$ nanoparticles, *International Journal of the Physical Sciences.*, 2011, 6, 6268-6279.

8. Martyshkin, D.V., V.V. Fedorov, C. Kim, I.S. Moskalev & S. Bmirov., Mid-IR random lasing of Cr-doped ZnS nanocrystals. Department of Physics, University of Alabama at Birmingham, 1300 University Boulevard, Birmingham, USA., 2010.
9. Ahmad, M., R. Kamran, I. Zahid, M. A. Rafiq & M. M. Hasan, 2011. Structural and Electrical properties of Zinc Sulfide Nanoparticles. Micro and Nano Devices Group, Department of Chemical and Materials Engineering, Pakistan Institute of Engineering and Applied Sciences Islamabad, Pakistan.
10. Lv J., W. Gong, K. Huang, J. Zhu, F. Meng, X. Song, Z. Sun., Effect of annealing temperature on photocatalytic activity of ZnO thin films prepared by sol-gel method. *Superlattices and Microstructures.*, 2011, 50, 98-106.
11. Barjasteh-Moghaddam, M. & A. Habibi-Yangjeh., Effect of Operational Parameters on Photodegradation of Methylene Blue on ZnS Nanoparticles Prepared in Presence of an Ionic Liquid as a Highly Efficient Photocatalyst, *Journal of the Iranian chemical society.*, 2011, 8:169-175.
12. Pouretedal, H.R., A. Norozi, M.H. Keshavarz & A. Semnani., Nanoparticles of zinc sulfide doped with manganese, nickel and copper as nanophotocatalyst in the degradation of organic dyes, *Journal of Hazardous Mater.*, 2009, 162, 674–681.
13. Saien, J. & S. Khezrianjoo, 2008. Degradation of the fungicide carbendazim in aqueous solutions with UV/TiO₂ process and optimization of kinetics and toxicity studies, *Journal of Hazardous Materials.*, 2008, 157, 269–276.
14. Amaranatha, R.D., G. Murali, R.P. Vijayalakshmi & B. K.Reddy, 2011. Room-temperature ferromagnetism in EDTA capped Cr-doped ZnS nanoparticles. *Journal of Applied physics.* 105:119–124.
15. Rahdar, A., E. Asnaasahri & R. Sarhaddi., Study of structural and optical properties of ZnS:Cr nanoparticles synthesized by co-precipitation method, *Journal of Indian Science and Technology.*, 2012, 5, 974- 6846.

.*****